Giovanni Vettori

NOVEL COMPOSITES OF PEDOT:PSS-PLATINUM NANOPARTICLES FOR CHEMIRESISTIVE BIOSENSORS

MASTER'S DEGREE THESIS

Supervised by Dr Jordi Riu Russell, Dr Ricard Boque and Dr Francisco J. Andrade

MASTER'S DEGREE IN NANOSCIENCE, MATERIALS AND PROCESSES:
CHEMICAL TECHNOLOGY AT THE FRONTIER (2022-23)

UNIVERSITAT ROVIRA i VIRGILI

Tarragona

2023

NOVEL COMPOSITES OF PEDOT:PSS-PLATINUM NANOPARTICLES FOR CHEMIRESISTIVE BIOSENSORS

Giovanni Vettori

Master’s Degree in Nanoscience, Materials and Processes: Chemical Technology at the Frontier (2022-23)

Supervised by Dr Jordi Riu Russell, Dr Ricard Boque and Dr Francisco J. Andrade

Universitat Rovira i Virgili, Department of Analytical Chemistry and Organic Chemistry

Campus Sescelades, Marcel·lí Domingo 1, Tarragona 43007, Spain

ABSTRACT

The use of chemiresistors for developing devices for the point-of-care is highly attractive because of their inherently compact and simple design. The basic chemiresistor architecture, consisting of two electrodes connected by an electronically conductive channel, is a key feature compared to other technologies such as organic electrochemical transistors (OECTs). In this work a paper-based chemiresistive sensor is proposed, in which the conductive channel consists of a PEDOT:PSS-Pt nanoparticles composite. The device has been optimized and tested first for the detection of hydrogen peroxide and later, after proper biofunctionalization with glucose oxidase enzyme, for the determination of glucose in aqueous environment. The system displayed a sensitivity of 8 Ω/decade towards both, peroxide and glucose, in the 0.03 – 1 mM and 0.3 – 10 mM linear ranges, respectively. The down scalability of the system has been tested by means of in-drop calibrations, resulting in a sensitivity of 6.7 Ω/dec with a linearity between 0.01 and 1 mM, proving the feasibility of operation in real scenarios.

1. INTRODUCTION

The increasing global attention to healthcare concerns emphasizes the importance of developing new point-of-care (POC) devices. The COVID-19 pandemic has further highlighted the significance of decentralized healthcare technologies, prompting increased research and production in this area.[1] Decentralized systems allow people to autonomously perform simple diagnostic tests by means of POC devices, offering numerous advantages. These include not only the possibility of self-administering more analyses, but also the reduction of unnecessary and time-demanding medical visits, avoiding potentially dangerous situations too. By enabling early diagnosis through the detection of suitable biomarker instead of waiting for the onset of symptoms, a predictive, preventive and personalized approach to medicine becomes also possible. Furthermore, in chronic conditions, the evolution of the health status may be easily and continuously monitored. Moreover, the widespread use of affordable and easily deployable point-of-care devices can help bridge the gap between high- and low-income countries, promoting diagnostics[2] strategies aligned with the UN sustainable and inclusive development goals. Currently, diabetes-focused devices such as the FreeStyle GCM System from Abbott[3] and the Glucometer from OrSense[4] dominate the market. However, a limitation of these products is that they focus solely on glucose monitoring. This deficiency becomes particularly relevant when considering the impact of other substances, such as alcohol consumption on glucose detection. Indeed, the presence of alcohol can interfere with the accuracy of glucose monitoring devices, producing false readings or signals that are difficult to distinguish.[5] Furthermore, the physical condition of the person may also have a significant impact on the prognosis of the disease. Thus, monitoring the levels of lactate in blood would provide valuable insights. Therefore, there is a need to address the limitations associated with single-analyte detection to provide more comprehensive and accurate care and advancing the field of decentralized diagnostics.

Pursuing the necessity of achieving multi-analyte detection, research on sensors arrays is active and evolving. The main approach relies on the combination of multiple individual sensors, each of them designed to interact with a specific analyte. These sensors can vary in their sensing mechanism and/or in the materials involved.[6–8] Several challenges must be addressed when developing an array of sensors: selectivity and sensitivity, in particular the difference in these parameters towards the analytes of interested, cross-reactivity and interference, data analysis and interpretation, miniaturization in integration in the final device.[9]

Electrochemical biosensors have traditionally showed significant recognition as analytical devices, particularly as tools for the point of need. Such tools display not only remarkable performances but also simple and cost-effective manufacturing, making them suitable for decentralized chemical analysis.[10,11] Among the several technologies in the field, chemiresistors appear to be remarkably promising. Chemiresistors are a subset of sensors that allow monitoring the change on the electrical resistance of an electron-conductive material depending on its chemical environment. In particular the conductivity of these materials is modulated by a recognition event with an analyte of interest. Such conductive material provides electrical connection between two electrodes forming the so-called channel and thus constituting the chemiresistive system. In broad terms, one of the main advantages of chemiresistors is the absence of an external reference electrode. Hence, in comparison with more complex technologies such as organic electrochemical transistors (OECTs), they allow simpler instrumental setups, i.e. involving a lower number of electrodes and connections.[12,13] Although the principle of chemiresistors is widely known, these type of systems have almost invariably been focused on gas sensing, mainly for industrial and environmental monitoring. The use of chemiresistors as bio-electrochemical sensors has been known for decades, but it has traditionally shown significant barriers. Instability, low reproducibility, as well as low sensitivity and selectivity, are significant aspects that must be improved for their application as POC devices.[14,15]

In the field of biosensors, conductive polymers are a well-established material of choice for electrodes channel fabrication.[16] The most commonly employed polymer of this kind is poly(3,4-ethylenedioxythiophene) doped with polystyrene sulfonate (PEDOT:PSS). PEDOT:PSS displays a set of remarkable properties from the high conductivity to its processability and stability. The particular interest in sensing applications is due to the ability of tuning its resistance according to its oxidation state: the electrical conductivity increases when the material is oxidized and decreases when reduced.[17] Moreover, PEDOT:PSS composites are also widely investigated thanks to the possibility of tailoring the properties and the applications of the final material. Nanomaterials such as platinum nanoparticles (Pt NPs), reduced graphene oxide, prussian blue and many others can be incorporated into the conductive polymer matrix to add catalytic activity towards a specific analyte.[18] The use of PEDOT:PSS allows also functionalization with biomolecules thanks to its biocompatibility: enzymatic layers may be involved in order to introduce a specific reaction with a molecule or compound of interest.[19]

Although research have been carried out,[15,20] an established knowledge about biomolecules detection by means of chemiresistive sensors is still yet to be achieved. In particular, chemiresistors based on PEDOT:PSS-composites need to be furtherly investigated and optimized.

Thus, the purpose of this project is to develop an array of three sensors for the simultaneous multi-analyte detection in biological samples. In particular, this preliminary work focuses on the optimization of the individual chemiresistors followed by their biofunctionalization. Lastly, downscaling the measurement setup may prove the feasibility of the system as a potential point-of-care device. The chemiresistors consists of two paper-based Au electrodes connected by a PEDOT:PSS-Pt nanoparticles composite channel. The functionalization with a glucose-oxidase enzymatic layer provides the desired bioactivity. The choice of the mentioned materials and biomolecules is justified by the aim of achieving a simple and cost-effective product and by the detection mechanism. This latter involves the production of hydrogen peroxide from the bioreaction occurring on the enzymatic layers when the analyte of interest is present. The catalytic activity of Pt nanoparticles towards H_2O_2 leads to a change in the oxidation state of PEDOT:PSS and therefore in its resistance. Using these reactions, this work presents the development and optimization of a novel paper-based chemiresistor for biochemical sensing with a very good sensitivity, selectivity and stability. This device shows promise as a future component of the point of care digital health toolbox.

2. EXPERIMENTAL

2.1. MATERIALS

All chemicals were analytical grade, purchased from Sigma–Aldrich (Merck, Spain). High conductivity grade PEDOT:PSS (3-4 %wt) in aqueous solution was used to fabricate the channel. Glucose oxidase (GOx, lyophilized powder from Aspergillus Niger Type X-S, 100-250 kU/g) and a 5 %wt Nafion® solution in aliphatic alcohols and water (45 % water) were used to functionalize the channel.

A H_2O_2 commercial stock solution 30 %(v/v) and D-(+)-Glucose were used to prepare the respective fresh standard solutions. 0.1 M Phosphate-buffered saline solution PBS at pH = 7.4 was prepared by dissolving Na_2HPO_4 0.100 M, KH_2PO_4 0.018 M, NaCl 0.1 M and KCl 0.003 M and suitable adjustment of the pH. All solutions were prepared using doubly deionized MilliQ water (MilliQ water systems, resistivity 18.2 MΩ/cm at 25 °C, SYNERGY® UV SYSTEMS, Merck KGaA, Darmstadt, Germany).

The Pt nanoparticles stabilized by triphenylphosphine (PPh_3) to be incorporated in the composite were provided by the Inorganic Chemistry group of URV, prepared according to reference[21].

Microporous lustre photography-quality paper (200 g/m^2; 200 ± 10 µm thick) purchased from a local supplier was used as a substrate for the chemiresistors.

2.2. INSTRUMENTATION

A Keithley 2100 Electrometer (Keithley Instruments, USA) was used to measure the resistance of the system. A Tenma 72-7720 Digital Multimeter (Tenma Electronics, Japan) was used to monitor daily the channel's static resistance in dry conditions. A CHI 660C Electrochemical Workstation (CH Instruments, USA) was used to perform cyclic voltammetry and chronopotentiometry. Transmission Electron Microscope (S/TEM) JEOL JEM F200 (JEOL, USA) and Field Emission Scanning Electron Microscope (FESEM) Scios™ 2 DualBeam (Thermo Scientific, USA) were used to characterize the composite film. A sputtering system ATC Orion UHV (AJA International Inc, USA) was used for the fabrication of the electrodes.

2.3. FABRICATION OF THE SENSORS

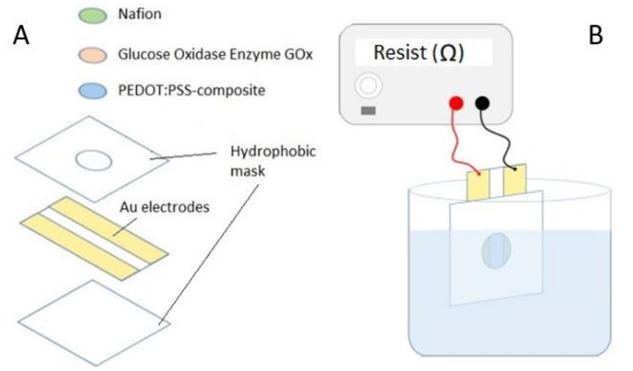

Figure 1. (A) Assembly of the chemiresistors with paper masks of 1.5x1.4 cm in size and Au-pads of 1.5x0.4 cm. (B) measurement setup in PBS background electrolyte solution.[12]

The fabrication method was based on previous works of the group.[10,12] In short, the electrode pads were created by sputtering a 100 nm Au layer on a paper substrate with a 0.5 mm wide adhesive tape in the middle. After sputtering, the tape was removed, leaving two electrodes separated by a 0.5 mm gap. These electrodes were then sandwiched in between two hydrophobic coated adhesive paper working as protective masks. The front mask has a 4 mm diameter window.

For creating the channel, a 0.1 %wt PEDOT:PSS aqueous solution was prepared by proper dilution of the commercial stock. A 5 mg/mL dispersion of Pt nanoparticles in THF was prepared and left sonicating for 10 min. Thereafter, the diluted PEDOT:PSS solution and the Pt dispersion were then mixed in a ratio 90:10 in volume, respectively, in an ultrasonic bath for 30 min. 3 µL of the obtained composite were drop cast to cover the window area and then soft baked at 100 °C for 20 min. Once cooled down to room temperature, 1 µL of dimethyl sulfoxide (DMSO) was deposited on the channel, soft baked again at 100°C for 5 min. Finally, the system was rinsed with MilliQ water. This last step is used as a conductivity enhancing treatment. The biofunctionalization of the channel was made by drop casting of 10 µL of GOx (20 mg/mL, in MilliQ water) then left it drying overnight in the fridge and drop casting 5 µL of Nafion®, left dry for 2h. (Figure 1A)

2.4. MICROSCOPY CHARACTERIZATION

The PEDOT:PSS-Pt composite was deposited and baked on a Si wafer and a lamella has been carved by Focused Ion Beam (FIB) to be transparent at the HRTEM. To cut a cross section, the device was fully coated with a 20nm Au layer and two Pt layers, 200 nm and 1.2 µm thick respectively, were further deposited to mark and protect the desired area. A 15 µm long and 5 µm deep cut was then performed by FIB. The section was then analysed at the FESEM.

2.5. ELECTROCHEMICAL CHARACTERIZATION

Cyclic voltammetry (CV) and chronopotentiometry (or galvanostatic charge-discharge, GCD) were both performed in KCl 0.1 M. To perform these experiments, the whole channel was used as working electrode, while a double junction Ag/AgCl electrode and a Pt wire were used as reference and counter electrodes, respectively. CV has been measured in the [-0.3 ; 0.3] V range, at a scan rate of 0.1 V/s. GCD has been measured between cutoff values of -0.1 and 0.3 V, applying a constant current of 10 µA. The specific capacitance has been estimated from the discharge segment of the CGD plot. The slope has been calculated from 4 points in the last 20s range of each curve (Δt of 5s). The so-obtained value has then been divided by the area of the window. Ohmic characteristics of the system were also studied by analysing the current vs voltage (I-V) output curves in PBS 0.1 M. For this experiment, the channel was placed in series of a feeding power supply line, and changes in the voltage were sequentially applied in a potential window from -0.4 to 0.4 V, in steps of 0.1 V.

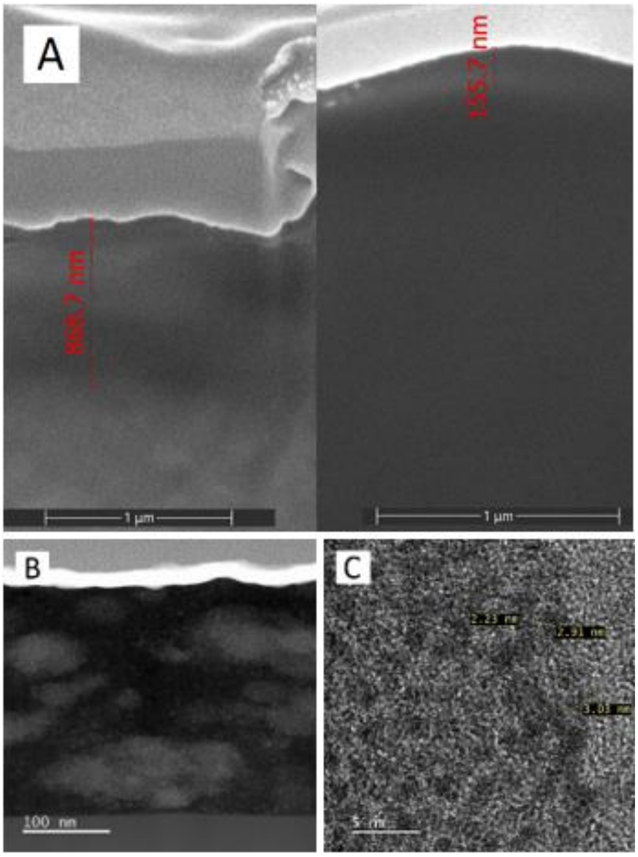

Figure 2. (A) FESEM cross-section images taken at the edges (LHS) and in the center (RHS) showing the thickness of the PEDOT:PSS layer, identified by the chromatic contrast and measured by the red lines. (B) HRTEM images of the PEDOT:PSS-Pt composite lamella (PEDOT:PSS 0.1 %wt, Pt 0.5 mg/mL) and (C) focus on the Pt NPs agglomerates.

2.6. ANALYTICAL PERFORMANCE

The channel resistance was monitored using a two-probe measurement setup with a Keithley 2100. The calibrations were performed both in solution and drop-based methods. In the first case, by immersion of the electrochemically active window in 5 mL of PBS under constant stirring, as showed in Figure 1B; in the second case, by deposition of a 10 µL drop of PBS to cover the whole window area.

3. RESULTS AND DISCUSSION

3.1. CHARACTERIZATION

3.1.1. CHARACTERIZATION OF THE COMPOSITE FILM

The conductive polymeric composite characteristics define the working principle of the chemiresistors. In particular, the thickness of the film and the size and distribution of the Pt nanoparticles are the main parameters to be investigated. Figure 2A shows the cross-section pictures cut by FIB and acquired by FESEM. The film appears to be unequally distributed along the window area: the cuts made at the edges and in the central region reveal thicknesses of 880 ± 70 and 130 ± 30 nm, respectively, suggesting an accumulation of the polymer towards the edges. This coffee-staining distribution happens often with the drop casting approach and is due to the minimization of the surface energy during the drying process. While some work has been performed to reduce this effect, it is not considered detrimental if it does not affect the reproducibility of the system. The size and dispersion of the incorporated Pt NPs have been verified by HRTEM. Irregular clouds of nanoparticles are distributed across all the material, with a variable size ranging from 10s to 100s of nanometres. (Figure 2B) The individual Pt NPs, recognized by the crystalline planes, display an estimated diameter of 2.6 ± 0.3 nm. (Figure 2C) The elemental EDS analysis, reported in Figure 3, further confirms the chemical nature of both

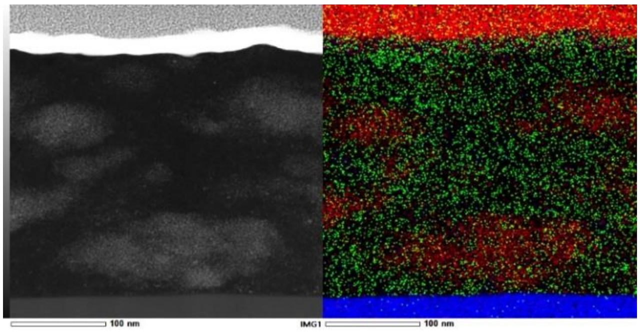

Figure 3. HRTEM image of the PEDOT:PSS-Pt composite (LHS) and corresponding EDS mapping (RHS) for the elements: S (green), Pt (red) and Si (blue).

matrix and nanoparticles, with the presence of sulphur coming from PEDOT:PSS and platinum.

3.1.2. ELECTRICAL CHARACTERIZATION

Cyclic voltammetry has been performed in the potential window from -0.3 to 0.3 V. The idea of this low range voltage is to explore whether electrochemical reactions catalysed by the composite may occur in regions close to 0 V, where the chemiresistor is intended to be used. Figure 4A shows the voltammograms obtained for the blank pristine PEDOT:PSS and for the PEDOT:PSS-Pt composite. Both systems display a quasi-rectangular shape, which is characteristic of an ideal capacitor, without relevant differences neither in shape nor in current intensity. This shape is due to the accumulation of charges through the formation of an electric double layer. The similarities between the systems suggest that the incorporation of Pt NPs does not affect the well-known highly capacitive behaviour of PEDOT:PSS.[22,23] Moreover, the absence of peaks shows that there is not Faradaic currents, providing further evidence against electron-transfer processes, e.g. of red-ox reactions, within the selected potential window. The capacitance of the pristine and composite materials has been furtherly evaluated by means of GCD measurements, as shown in Figure 4B. A slight asymmetric drift can be observed in the charging phase when reaching higher potentials. Nevertheless, the overall symmetry of the charge and discharge slopes confirms the capacitive nature of PEDOT:PSS. The estimated capacitance of PEDOT:PSS and its Pt composite, calculated from the slope of the discharge segment resulted to be 6.7 and 5.4 mF/cm^2, respectively.

The output curves time traces shown in Figure 4C display a significant degree of linearity evidencing a clear ohmic behaviour of the materials. Forward and backward scanning show no hysteresis effects or ageing. Figure 4D shows the I-V linearized plots with the claculated slopes. It can be seen that the addition of the Pt NPs produces a slight increase of the slope, i.e., decrease of the resistance of the material.

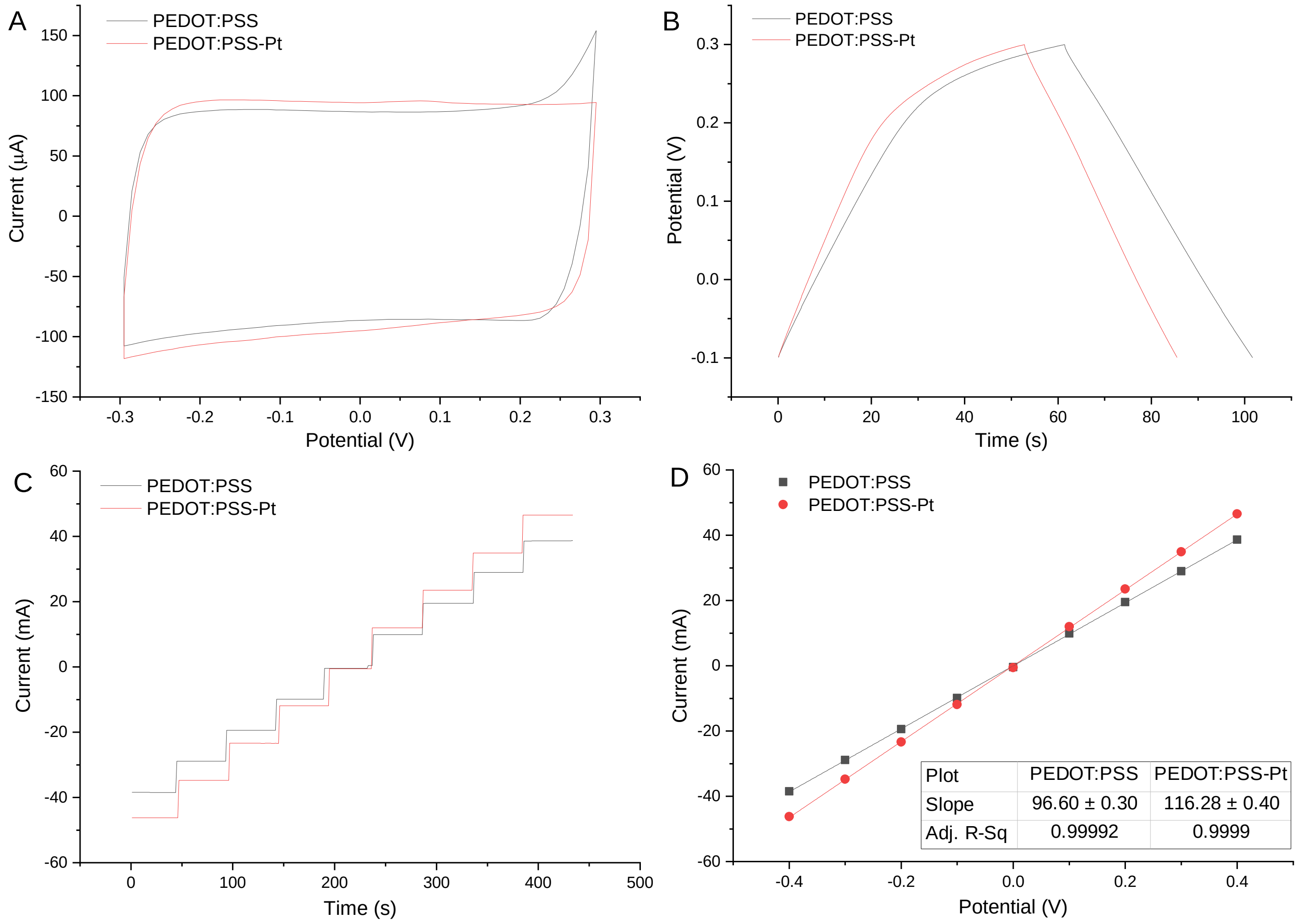

Figure 4. Electrical characterization of pristine PEDOT:PSS and PEDOT:PSS-Pt. (A) Cyclic voltammograms between -0.3 and 0.3 V in KCl 0.1M. (B) Charge-discharge measurements between -0.1 and 0.3 V (I = 10 µA) (C) Output curve of ohmic time traces between -0.4 and 0.4 V, ΔV=0.1V in PBS 0.1M and (D) corresponding calculated I-V curves.

3.2. ANALYTICAL PERFORMANCE

3.2.1. H_2O_2 DETECTION AND CHANNEL OPTIMIZATION

The main goal of this work is to develop a material whose electrical resistance responds to the presence of a relevant chemical substance. Peroxide is chosen as a target since this molecule is present in a plethora of direct and indirect bioassays. The main hypothesis is that, while PEDOT:PSS is virtually unsensitive to peroxide, the addition of Pt can sensitize the material. To prove this point, experiments were performed using blank (no Pt NPs) and functionalized channel. These results are summarized in Figures 5A-C. As expected, the blank test performed on pristine PEDOT:PSS, i.e. without Pt NPs incorporation, displayed a small response showing a decrease in electrical resistance likely due to the oxidation of the material triggered by the presence of peroxide. Conversely, when Pt is present, two main changes occur. First, the increasing concentration of H_2O_2 leads to an increase in electrical resistance. This behaviour points to the opposite red-ox mechanism and therefore to the conversion of PEDOT:PSS in its reduced and less conductive form. Second, the magnitude of the changes is significantly higher than in the blank system.

The phenomena observed is likely due to the catalytic activity of Pt NPs towards H_2O_2. It has been shown that peroxide has a two-step mechanism involving first the oxidation of Pt to PtO[24] and the subsequent PtO-surface mediated oxidation reaction of peroxide. Once this happens, the system is balanced by the reduction reaction of PEDOT:PSS. While more work should be devoted to study the actual mechanism, these first results work as a proof of principle for the detection of peroxide. Evidently, the morphology and features of the polymeric layer play a crucial role in the performances of the chemiresistors. Optimization of the analytical parameters was pursued by evaluating the influence of several variables, namely: window diameter and deposited PEDOT:PSS-Pt composite volume. Also, approaches to improve the drop casting technique by manually spreading the drop with the help of the pipette tip to cover all the area were tested. Table 1 reports the mean values of the initial channel resistance in solution and the to peroxide sensitivity calculated from the calibration curves of the several tested combinations.

The optimal parameters were selected in terms of sensitivity and reproducibility of the sensors.

Table 1. Initial resistance (Ri, baseline value before the calibration in solution), sensitivity and R^2 value for the window diameters (D_{wind}) and composite volumes (V_{comp}) tested. (drop cast without any manual spreading).*

d_{wind} (mm)	V_{comp} (µL)	Ri (Ω)	Sensitivity (Ω/decade)
4	4	290 ± 50	19 ± 7
4	3	1400 ± 900	50 ± 70
4	3*	190 ± 40	7 ± 4
3	4	200 ± 70	10 ± 10
3	**3**	**220 ± 40**	**8 ± 4**
2.5	3*	120 ± 20	2.3 ± 0.6

A window diameter of 3 mm and a cocktail volume of 3 µL were chosen. This provides a mean initial resistance of 220 ± 40 Ω and a sensitivity of 8 ± 4 Ω/decade. The low wettability of the surface might be the reason why the sole drop deposition, i.e., without any auxiliary spreading, is not optimal. Indeed, a significant portion of Au surface always remained exposed to the environment, especially when dealing with larger window diameters such as 4 mm. This could possibly cause additional and not controlled interaction phenomena, leading therefore to not reproducible results. On the other hand, the manual spreading represents a significant source of human errors determined by the possibility of damaging the delicate Au layer. The high variability registered in both resistance and sensitivity can be related to several factors: from the non-homogeneous dispersion of the Pt NPs in the PEDOT:PSS matrix to the unequal distribution of the film itself in terms of thickness along the window area. Moreover, a correlation between initial resistance and sensitivity can be observed: the higher the first the higher the latter, even if linear fit cannot be identified.

Figure 5 displays the time traces (A) and the respective calibration curves (B), showing the response of the selected chemiresistors to additions of H_2O_2. Three consecutive calibrations of two sensors are reported, with H_2O_2 from $1x10^{-3}$ to 1 mM (-6 to -3 in logarithmic scale). All the sensing performance tests here reported were conducted on the PEDOT:PSS-Pt based chemiresistors. The calculated sensitivities were 5 ± 1 Ω/dec and 10.9 ± 0.9 Ω/dec in the [-4.5; -3] and [-5; -3] log-linear ranges, respectively. The low standard deviations, calculated for both initial resistance and sensitivity between consecutive calibrations, stress the ability of the system to recover the initial baseline as well as the repeatability among consecutive measurements. (Table 2) These have also been proven in a repeatability test, where single peroxide additions, at a concentration of -5, were made and then washed with PBS. Figure 6 shows how comparable the ΔR was among the three consecutive tests, enlightened by the thicker line. On top of this, the baseline is shown to be always recovered. The corresponding data are reported in Table 3.

3.2.2. GLUCOSE DETECTION IN SOLUTION

Once the detection of peroxide has been optimized, the system has been functionalized through the addition of a GOx and a Nafion® layer in order to introduce bioactivity and selectivity towards glucose.

Table 2. Initial resistance and sensitivity, with corresponding standard deviation (σ), and linear range of consecutive H_2O_2 and Glucose calibrations.

		Calib n	Ri (Ω)	σ_{Ri} (Ω)	Sens (Ω/dec)	σ_{Sens} (Ω/dec)	L.R. (mM)
Peroxide	Sensor 1	C1	179.4	1.5	4.01	1.16	0.01 – 1
		C2	176.6		5.41		0.01 – 1
		C3	177.1		6.31		0.01 – 1
	Sensor 2	C1	288.3	0.0	10.02	0.90	0.03 – 1
		C2	288.3		11.81		0.03 – 1
		C3	288.3		11.03		0.03 – 1
Glucose	Sensor 3	C1	232.9	2.2	7.84	1.57	0.3 – 3
		C2	229.5		10.07		0.3 – 10
		C3	228.7		10.87		0.3 – 10
	Sensor 4	C1	200.3	1.9	5.73	0.39	0.3 – 10
		C2	203.8		5.92		0.1 – 10
		C3	203.4		6.49		0.1 – 10

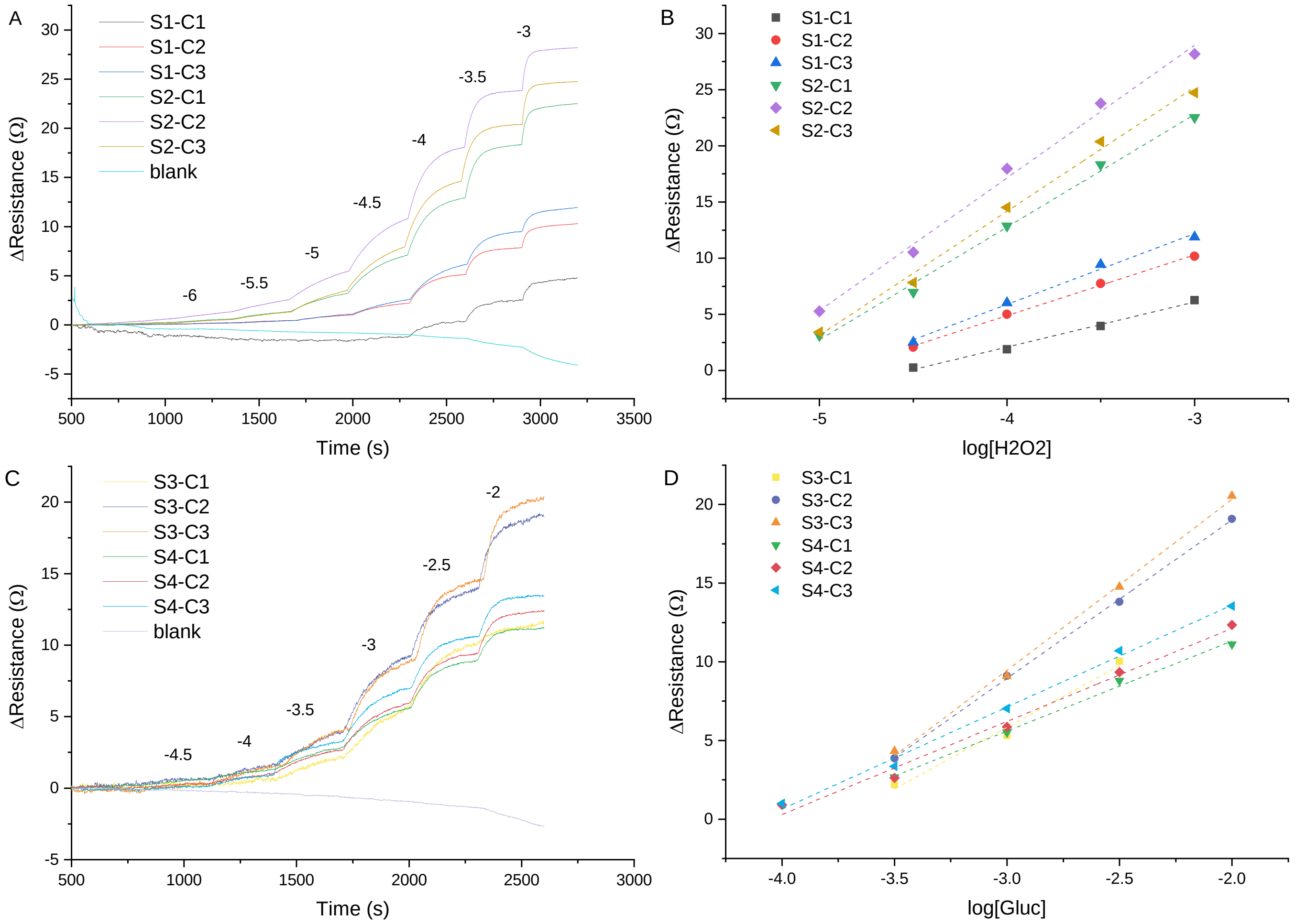

Figure 5. (A) Consecutive time traces and (B) corresponding calibration curves in resistance as response to H_2O_2 additions from -6 to -3 (+0.5 every 300s). (C) Consecutive time traces and (D) corresponding calibration curves in resistance as response to glucose additions from -4.5 to -2 (+0.5 every 300s). The blank refers to the absence of Pt NPs incorporation.

Table 3. Resistance at the moment of the addition (R_{add}), resistance increase (ΔR) and corresponding σ values.

Add	R_{add} (Ω)	σ_R (Ω)	ΔR (Ω)	$\sigma_{\Delta R}$ (Ω)
1	280.6	1.9	7.0	2.2
2	277.3		9.7	
3	277.1		11.4	

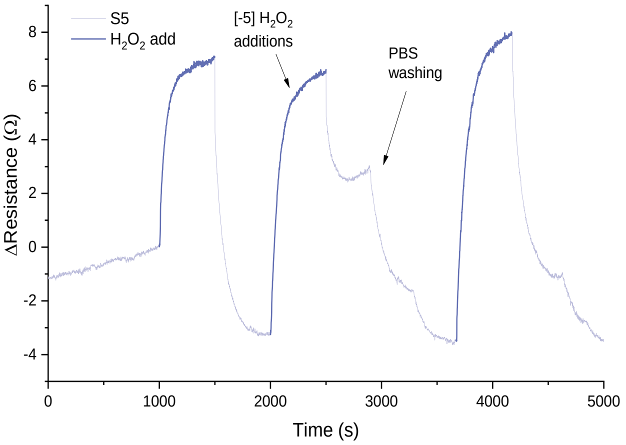

Figure 6. Repeatability of the response to 0.01 mM (-5) H_2O_2 additions and recovery of the baseline by PBS washing after 500s from the additions.

This latter is oxidised by O_2 in the presence of GOx according to the following bioreaction:

$$\text{D–glucose} + O_2 \rightarrow \text{D-glucono-1,5-lactone} + H_2O_2$$

Peroxide is therefore generated as by-product directly on the surface of the channel, triggering a sensing response comparable to what has been previously reported. The same analytical performance test has been carried on and three consecutive calibrations of two functionalized chemiresistors are reported in Figure 5C and 5D. Here, instead of peroxide, the glucose concentration has been increased from 0.032 to 10 mM (-4.5 to -2 in logarithmic scale) and the response has been evaluated. The mean sensitivities of the two sensors were 10 ± 2 Ω/dec and 6.1 ± 0.4 Ω/dec in the respective linear ranges of [-4 ; -2] and [-3.5 ; -2]. Once again, the repeatability of the system is demonstrated by the low σ values. (Table 2) In both the sensors here reported, an increase in sensitivity as well as an extension of the linear range can be observed when moving to the second and third calibrations. This suggest that an activation through a pre-conditioning in a 10 mM glucose solution might be introduced in the experimental routine. The obtained linear range covers well the glucose concentration range in blood, typically between 4 and 7 mM (-2.4 to -2.1 in log scale).[25] This would allow a direct measurement in plain blood without the need of sample dilutions.

3.2.3. GLUCOSE DETECTION IN A DROP

In order to verify the down-scalability of the system, the experimental setup has been slightly readapted. Instead of immersing the chemiresistors in solution, the same performance test has been conducted in a 10 µL drop, to simulate the analysis of a realistically smaller sample volume. This experiment was made possible by one of the advantages of the chemiresistor: the absence of an external reference or a gate electrode, which allow an extremely compact setup. Indeed, only the channel window needs to be covered by the sample and the volume is hence defined by the diameter, allowing a further miniaturization of the whole system.

The sensor has been positioned horizontally and a 10 µL drop of 0.1 M PBS has been deposited to cover the window. The response to glucose additions from 10^{-3} to 1 mM (-6 to -3 in log scale) has been evaluated and compared to the one previously obtained in solution. As shown in Figure 7, the calculated sensitivity turned out to be 6.7 ± 0.2 Ω/dec in the linear range [-5 ; -3]. As a preliminary conclusion, direct measurement in sweat could also be achieved since the normal glucose concentration in sweat typically ranges from 0.06 to 0.2 mM (-4.2 and -3.7 in log scale).[26] The shape of the time trace obtained from the in-drop calibration suggests a slower and less marked response, especially at lower concentrations. Such behaviour might be attributed to the lack of stirring. Despite of this, the glucose sensing performance is comparable to the one registered in solution. Considering a mean sensitivity of 8 ± 2 Ω/dec, the obtained value perfectly lies in the uncertainty range.

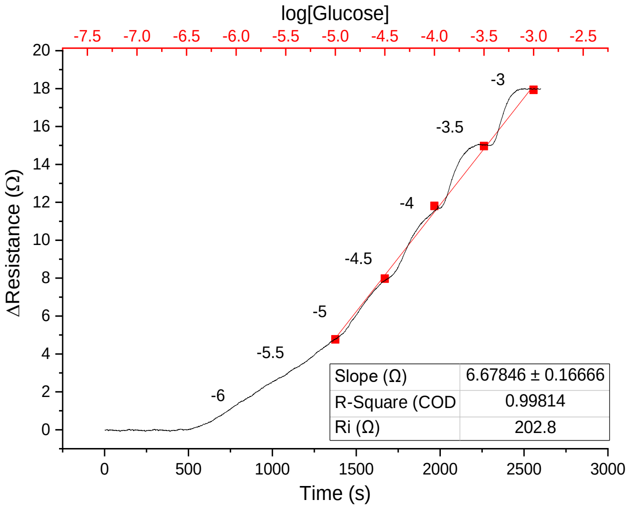

Figure 7. Time trace (black) and corresponding calibration curve (red) in resistance as response to glucose additions (log scale) in a 10 µL drop of PBS 0.1 M.

4. CONCLUSIONS AND FUTURE WORK

In this work, an easily manufacturable sensing device has been optimized and its analytical performances have been reported. The chemiresistor technology allows to employ a simple measurement setup and the paper-based components make the fabrication process easy and cost-effective since no sophisticated techniques are required. The properties of the device are attributed to the conductive polymeric composite channel, consisting of a 0.1 %wt PEDOT:PSS matrix including Pt NPs in a concentration of 0.5 mg/mL. After characterizing the system from a morphological and electrochemical point of view, the optimal fabrications features have been evaluated, selecting a 3 mm channel window and a composite volume of 3 µL. The device has first been tested in response to peroxide obtaining a sensitivity in the order of 10 Ω/decade, with a linearity fluctuating between -5/-4.5 and -3, in logarithm of peroxide concentration. Glucose, as analyte of interest, has then been detected by adding a glucose oxidase layer, with the purpose of producing H_2O_2 as by-product of the enzymatic conversion. The performance of the functionalized sensor has been evaluated both in solution and in a 10 µL drop, obtaining again a sensitivity in the order of 10 Ω/decade. The linear range for glucose detection in solution turned out to be slightly shifted towards higher concentration, in respect to peroxide detection, ranging between -4/-3.5 and -2. The in-drop test gave promising results in the -5 to -3 linear range, with a sensitivity comparable to the one obtained in the 5 mL cell solution, but in a 500 times lower volume. Thanks to the advantageous architecture of the chemiresistor, downscalability is therefore a feasible path to follow for the proposed system in the perspective of a point-of-care device where the sample to be analysed would possibly consist of a small drop. Direct measurement in whole blood would be possible, since the typical concentration range is covered by the obtained linear ranges. Moreover, detection in sweat could be also achieved after further investigation, which would be a an interesting application due to the easier and less invasive collection process. In all these cases, studies of the matrix effect still need to be conducted.

Further experiments are needed to investigate the optimal deposition conditions and/or technique, which perhaps may be different from the manual drop casting adopted in this work. Achieving a more homogeneous dispersion of the Pt NPs in the matrix and an equal distribution of the film all over the window area might be the key to reduce the fluctuations encountered in terms of resistance and sensitivity, leading to a higher reproducibility.

Future work should then involve the combination of multiple chemiresistors to achieve multianalyte detection. An array of three sensors would for instance allow to independently detect two analytes at the same time in a sample, just by introducing selectivity towards different biomolecules such as glucose, lactate and alcohol. A blank sensor to constantly monitor the matrix would also be included in the system. Furthermore, an array of sensors for the same analyte could be designed with the purpose of extending the linear range and/or improving the precision of the device.

5. ACKNOWLEDGEMENTS

I would like to thank my supervisors Dr Francisco J. Andrade and Dr Jordi Riu Russell as well as Dr Pascal Blondeau for their precious counselling during this work and for their support and motivation in pursuing the highest objectives. I would also like to mention the valuable assistance and advice received from my colleagues Andres and Marc.

REFERENCES

(1) Wang, C.; Liu, M.; Wang, Z.; Li, S.; Deng, Y.; He, N. Point-of-Care Diagnostics for Infectious Diseases: From Methods to Devices. *Nano Today* **2021**, *37*, 101092. https://doi.org/10.1016/j.nantod.2021.101092.

(2) Vashist, S. K. Point-of-Care Diagnostics: Recent Advances and Trends. *Biosensors* **2017**, *7* (4), 62. https://doi.org/10.3390/bios7040062.

(3) Bidonde, J.; Fagerlund, B. C.; Frønsdal, K. B.; Lund, U. H.; Robberstad, B. *FreeStyle Libre Flash Glucose Self-Monitoring System: A Single-Technology Assessment*; NIPH Systematic Reviews; Knowledge Centre for the Health Services at The Norwegian Institute of Public Health (NIPH): Oslo, Norway, 2017.

(4) Amir, O.; Weinstein, D.; Zilberman, S.; Less, M.; Perl-Treves, D.; Primack, H.; Weinstein, A.; Gabis, E.; Fikhte, B.; Karasik, A. Continuous Noninvasive Glucose Monitoring Technology Based on “Occlusion Spectroscopy.” *J. Diabetes Sci. Technol.* **2007**, *1* (4), 463–469. https://doi.org/10.1177/193229680700100403.

(5) Emanuele, N. V.; Swade, T. F.; Emanuele, M. A. Consequences of Alcohol Use in Diabetics. *Alcohol Health Res. World* **1998**, *22* (3), 211–219.

(6) Jiang, Y.; Tang, N.; Zhou, C.; Han, Z.; Qu, H.; Duan, X. A Chemiresistive Sensor Array from Conductive Polymer Nanowires Fabricated by Nanoscale Soft

Lithography. *Nanoscale* **2018**, *10* (44), 20578–20586. https://doi.org/10.1039/C8NR04198A.

(7) Bohrer, F. I.; Covington, E.; Kurdak, Ç.; Zellers, E. T. Characterization of Dense Arrays of Chemiresistor Vapor Sensors with Submicrometer Features and Patterned Nanoparticle Interface Layers. *Anal. Chem.* **2011**, *83* (10), 3687–3695. https://doi.org/10.1021/ac200019a.

(8) Johnson, K. J.; Rose-Pehrsson, S. L. Sensor Array Design for Complex Sensing Tasks. *Annu. Rev. Anal. Chem. Palo Alto Calif* **2015**, *8*, 287–310. https://doi.org/10.1146/annurev-anchem-062011-143205.

(9) Askim, J. R.; Suslick, K. S. Colorimetric and Fluorometric Sensor Arrays for Molecular Recognition. In *Comprehensive Supramolecular Chemistry II*; 2017. https://doi.org/10.1016/B978-0-12-409547-2.12616-2.

(10) Estivill, M.; Ait Yazza, A.; Blondeau, P.; Andrade, F. High-Performance Ion-Selective Organic Electrochemical Transistors for the Determination of Potassium in Clinical Samples. *SSRN Electron. J.* **2022**. https://doi.org/10.2139/ssrn.4157202.

(11) Yogeswaran, U.; Chen, S.-M. A Review on the Electrochemical Sensors and Biosensors Composed of Nanowires as Sensing Material. *Sensors* **2008**, *8* (1), 290–313. https://doi.org/10.3390/s8010290.

(12) Ait Yazza, A. New Organic Electrochemical Sensing Platforms For The Point-Of-Need. Ph.D. Thesis, Universitat Rovira i Virgili, 2022. https://www.tdx.cat/handle/10803/687504 (accessed 2023-07-06).

(13) Ait Yazza, A.; Blondeau, P.; Andrade, F. J. Simple Approach for Building High Transconductance Paper-Based Organic Electrochemical Transistor (OECT) for Chemical Sensing. *ACS Appl. Electron. Mater.* **2021**, *3* (4), 1886–1895. https://doi.org/10.1021/acsaelm.1c00116.

(14) Koo, W.-T.; Jang, J.-S.; Kim, I.-D. Metal-Organic Frameworks for Chemiresistive Sensors. *Chem* **2019**, *5* (8), 1938–1963. https://doi.org/10.1016/j.chempr.2019.04.013.

(15) Song, E.; Costa, T. H.; Choi, J.-W. A Chemiresistive Glucose Sensor Fabricated by Inkjet Printing. *Microsyst. Technol.* **2017**, *23* (8), 3505–3511.

(16) Sharma, S.; Sudhakara, P.; Omran, A. A. B.; Singh, J.; Ilyas, R. A. Recent Trends and Developments in Conducting Polymer Nanocomposites for Multifunctional Applications. *Polymers* **2021**, *13* (17), 2898. https://doi.org/10.3390/polym13172898.

(17) Zhang, X.; Yang, W.; Zhang, H.; Xie, M.; Duan, X. PEDOT:PSS: From Conductive Polymers to Sensors. *Nanotechnol. Precis. Eng. NPE* **2021**, *4* (4), 045004. https://doi.org/10.1063/10.0006866.

(18) Chang, L.-C.; Wu, H.-N.; Lin, C.-Y.; Lai, Y.-H.; Hu, C.-W.; Ho, K.-C. One-Pot Synthesis of Poly (3,4-Ethylenedioxythiophene)-Pt Nanoparticle Composite and Its Application to Electrochemical H2O2 Sensor. *Nanoscale Res. Lett.* **2012**, *7* (1), 319. https://doi.org/10.1186/1556-276X-7-319.

(19) Kaur, G.; Adhikari, R.; Cass, P.; Bown, M.; Gunatillake, P. Electrically Conductive Polymers and Composites for Biomedical Applications. *RSC Adv.* **2015**, *5* (47), 37553–37567. https://doi.org/10.1039/C5RA01851J.

(20) Giaretta, J.; Oveissi, F.; Dehghani, F.; Naficy, S. Paper-Based, Chemiresistive Sensor for Hydrogen Peroxide Detection. *Adv. Mater. Technol.* **2021**, *6*. https://doi.org/10.1002/admt.202001148.

(21) Gil Jiménez, L.; Vicente Valverde, I.; Gual Gozalbo, A.; Godard, C.; Claver Cabrero, C. Alkane Dehydrogenation Nanocatalyst and Process For Its Preparation. WO/2022/180125, February 23, 2022. https://www.sumobrain.com/patents/WO2022180125A1.html.

(22) Volkov, A. V.; Wijeratne, K.; Mitraka, E.; Ail, U.; Zhao, D.; Tybrandt, K.; Andreasen, J. W.; Berggren, M.; Crispin, X.; Zozoulenko, I. V. Understanding the Capacitance of PEDOT:PSS. *Adv. Funct. Mater.* **2017**, *27* (28), 1700329. https://doi.org/10.1002/adfm.201700329.

(23) Manjakkal, L.; Pullanchiyodan, A.; Yogeswaran, N.; Hosseini, E. S.; Dahiya, R. A Wearable Supercapacitor Based on Conductive PEDOT:PSS-Coated Cloth and a Sweat Electrolyte. *Adv. Mater.* **2020**, *32* (24), 1907254. https://doi.org/10.1002/adma.201907254.

(24) Serra-Maia, R.; Bellier, M.; Chastka, S.; Tranhuu, K.; Subowo, A.; Rimstidt, J. D.; Usov, P. M.; Morris, A. J.; Michel, F. M. Mechanism and Kinetics of Hydrogen Peroxide Decomposition on Platinum Nanocatalysts. *ACS Appl. Mater. Interfaces* **2018**. https://doi.org/10.1021/acsami.8b02345.

(25) Cánovas, R.; Blondeau, P.; Andrade, F. J. Modulating the Mixed Potential for Developing Biosensors: Direct Potentiometric Determination of Glucose in Whole, Undiluted Blood. *Biosens. Bioelectron.* **2020**, *163*, 112302. https://doi.org/10.1016/j.bios.2020.112302.

(26) Zafar, H.; Channa, A.; Jeoti, V.; Stojanović, G. M. Comprehensive Review on Wearable Sweat-Glucose Sensors for Continuous Glucose Monitoring. *Sensors* **2022**, *22* (2), 638. https://doi.org/10.3390/s22020638.